

1

## Supporting Information

2

### 3 Tuning the distribution of Al atoms in the framework of Beta

4 zeolite and impact on the alkylation of phenol

5 **Zhuo Zhang<sup>a</sup>, Huoyan Jiang<sup>a</sup>, Yi Huang<sup>c</sup>, Baoyu Liu<sup>\*,a,b</sup>**

6 <sup>a</sup>School of Chemical Engineering and Light Industry, Guangdong University of Technology, Guangzhou, 510006,  
7 P.R. China

8 <sup>b</sup>Guangdong Provincial Laboratory of Chemistry and Fine Chemical Engineering Jieyang Center, Jieyang 515200,  
9 China

10 <sup>c</sup>School of Engineering, Institute for Materials & Processes, the University of Edinburgh, Edinburgh EH9 3FB,  
11 United Kingdom

12

13

14

15

16

17

18

19

20

21

22

23

24

25

26

### 27 Table of Contents

---

\* Corresponding author, Email: [baoyu.liu@gdut.edu.cn](mailto:baoyu.liu@gdut.edu.cn) (Baoyu Liu)

1	
2	<b>Experimental Procedures</b> .....S3
3	<b>Materials</b> .....S3
4	<b>Catalyst characterization</b> .....S3
5	<b>Catalytic tests</b> .....S4
6	<b>Figures and Tables</b> .....S6
7	<b>Figure S1.</b> SEM images of Beta-H (a and b), Beta-C (c and d), Beta-N (e and f). .....S6
8	<b>Figure S2.</b> Nitrogen adsorption-desorption isotherms of the obtained Beta zeolites. .....S6
9	<b>Figure S3.</b> UV-vis spectra of different dehydrated Co-Beta zeolites. .....S7
10	<b>Figure S4.</b> Representation of Beta zeolite framework in the [010] axis with nine different T-sites substituted by $\text{Al}^{3+}$ ion (Si yellow, Al red, O blue, H white). .....S7
11	
12	<b>Figure S5.</b> Product distributions with time-on-stream over (a) Beta-H, (b) Beta-C and (c) Beta-N, respectively. .....S8
13	
14	<b>Figure S6.</b> Thermogravimetric (TG) curves of various spent Beta zeolites. .....S9
15	<b>Figure S7.</b> Quantitative relationship between concentrations of different aluminum species
16	and Brønsted acid sites (BAS) and phenol conversion(all provided data were evaluated at 353
17	K and 1 h, with a ratio of phenol and <i>tert</i> -butanol to 2:1 ) .....S9
18	<b>Table S1.</b> Acid density of Beta zeolite catalysts.....S10
19	<b>Table S2.</b> The distribution of Brønsted acid sites in Beta zeolites .....S10
20	<b>Table S3.</b> Coke deposit of resultant Beta zeolites. .....S10
21	<b>References</b> .....S11
22	
23	
24	
25	

## 1 Experimental Procedures

## 2 Materials

3 The chemical regents used in present research involve JN-30 silica sol (30 wt%,  
4 Qingdao Haiwan Chemical Co., Ltd), sodium aluminate (53 wt% Al<sub>2</sub>O<sub>3</sub>, 42 wt% Na<sub>2</sub>O,  
5 Macklin), Tetraethylammonium hydroxide (TEAOH, 35 wt%, Macklin),  
6 Tetraethylammonium chloride (TEACl, 98%, Macklin), Tetraethylammonium nitrate  
7 (TEANO<sub>3</sub>, 98%, Macklin), sodium hydroxide (NaOH, 96%, Macklin), ammonium  
8 chloride (NH<sub>4</sub>Cl, 99 wt%, Tianjin Damao Chemical Reagent Co.), cobaltous nitrate  
9 (Co(NO<sub>3</sub>)<sub>2</sub>·6H<sub>2</sub>O, 99 wt%, Macklin), phenol (99.5%, Macklin), *tert*-butanol (AR,  
10 Macklin), n-dodecane (AR, Macklin), cyclohexane (AR, Macklin), pyridine (AR,  
11 Macklin), 2,4,6-trimethylpyridine (AR, Macklin), deionized water.

## 12 Catalyst characterization

13 The crystal structures of prepared zeolites were characterized by X-ray diffraction  
14 (XRD) analyzer that was conducted on a Bruker-AXS D2 PHASER Advance  
15 diffractometer with Cu K $\alpha$  radiation. The morphology of the zeolites was observed by  
16 a TDCLS-4800 scanning electron microscope (SEM). The amounts of silicon,  
17 aluminum and cobalt in the zeolite materials were determined by inductively coupled  
18 plasma optical emission spectroscopy (ICP-OES). The textural parameters of Beta  
19 zeolites were measured by Micromeritics ASAP 2460 devices at 77 K, and zeolites  
20 were pretreated under the condition of 473 K and vacuum for 6 h. The total surface area  
21 of the resultant samples was determined by the Brunauer-Emmett-Teller (BET) model,  
22 while the pore size distribution was obtained by the Barrett-Joyner-Halenda (BJH)  
23 model based on N<sub>2</sub> desorption isotherm. The total density of acid sites was determined  
24 by Fourier transform infrared spectroscopy with the probe molecules of pyridine, using  
25 a Bruker VERTEX 70 spectrometer. The zeolites were firstly degassed at 723 K for 2  
26 h before the measurements, then pyridine was adsorbed on the zeolites for 0.5 h at 298  
27 K. Secondly, the temperature was raised to 423 K at 1 h to remove the weakly bound  
28 pyridine molecules. Thirdly, the acid density of resultant zeolites was measured by  
29 infrared spectroscopy at 32 scans and a resolution of 2 cm<sup>-1</sup> when these samples were  
30 cooled to 298 K. In the Py-IR spectra, the characteristic peak of Brønsted acid and

1 Lewis acid sites for zeolite are at  $1545\text{ cm}^{-1}$  and  $1455\text{ cm}^{-1}$ , respectively. The molar  
2 extinction coefficient of  $2.22\text{ cm }\mu\text{mol}^{-1}$  and  $1.67\text{ cm }\mu\text{mol}^{-1}$  were used to calculate the  
3 density of Brønsted acid sites and Lewis acid sites, respectively. In the FT-IR spectra  
4 of adsorbed 2,4,6-trimethylpyridine, the characteristic peak of Brønsted acid sites is at  
5  $1636\text{ cm}^{-1}$ , corresponding to a molar extinction coefficient of  $10.1\text{ cm }\mu\text{mol}^{-1}$ .<sup>1,2</sup> In  
6 addition, the acidity of obtained samples were also measured by temperature  
7 programmed desorption of ammonia (NH<sub>3</sub>-TPD) on an AutoChem 2920 instrument  
8 equipped with a thermal conductivity detector (TCD). The high-resolution <sup>27</sup>Al MAS  
9 NMR characterizations were performed to determine the Al coordination environment  
10 on a Bruker Avance Neo 400WB spectrometer equipped at a resonance frequency of  
11 104.3 MHz. The measurements were performed on non-hydrated samples using a pulse  
12 length of  $3.84\text{ }\mu\text{s}$  and a power of  $95.91\text{ W}$ . The spectral data were fitted and analyzed  
13 using the Mastrenova.15. Diffuse reflectance ultraviolet-visible (UV-vis) spectra of the  
14 dehydrated Co-Beta-H, Co-Beta-C, and Co-Beta-N samples were measured against  
15 BaSO<sub>4</sub> in the range of 200-600 nm on a Shimadzu UV3700i spectrometer. Before each  
16 measurement, the hydrated Co-Beta-X samples were dehydrated for 3 h at  $10^{-1}\text{ Pa}$  and  
17 723 K in order to eliminate the influence of divalent cobalt species with H<sub>2</sub>O or  
18 hydroxyl groups.<sup>3</sup>

19 **Catalytic tests**

20 The catalytic performances of resultant Beta zeolites in the alkylation of phenol  
21 with *tert*-butanol were evaluated in a three-necked round-bottom flask under  
22 atmospheric pressure at 353 K. In a typical reaction, 0.2 g of zeolite was employed, the  
23 molar ratio of phenol and *tert*-butanol was 1:2. Specially, the cyclohexane was served  
24 as the solvent, while *n*-dodecane was functioned as the internal standard substance. The  
25 reaction mixture was periodically taken and analyzed by gas chromatograph equipped  
26 with an HP-5 column and a flame ionization detector.

27 Subsequently, their stability and lifetime were further investigated through a fixed-  
28 bed reactor, and a 10 mm diameter reactor tube was used. The reaction was carried out  
29 under atmospheric pressure at 413 K. All Beta zeolite catalysts were pelletized to a size  
30 of 20-40 mesh and activated at 673 K for 4 h prior to testing. The molar ratio of phenol

1 to *tert*-butanol was 1:2 and a total weight hourly space velocity (WHSV) was 5 h<sup>-1</sup>,  
2 these products were collected every 2 h and analyzed by gas chromatography as  
3 mentioned above. Prior to testing, all Beta zeolites were ion-exchanged three times at  
4 353 K for 12 h, using 1.0 mol L<sup>-1</sup> NH<sub>4</sub>Cl aqueous solution, and these Beta zeolites were  
5 transformed into H<sup>+</sup> form.<sup>4</sup> The conversion of phenol and the selectivity of 4-TBP were  
6 calculated according to specific formulas<sup>2</sup>:

7

$$\text{Conversion of Phenol} = \left(1 - \frac{C_A}{C_{A,0}}\right) \times 100\% \quad (1)$$

$$\text{Selectivity of 4-TBP} = \left( \frac{n_{4-TBP}}{n_{TBPE} + n_{2-TBP} + n_{4-TBP} + n_{2,4-DTBP} + n_{2,6-DTBP} + n_{2,4,6-TTBP}} \right) \times 100\% \quad (2)$$

8

9 where  $C_{A,0}$  is the initial concentration of phenol in the mixtures (mmol L<sup>-1</sup>) and  $C_A$  is  
10 the concentration of phenol after reaction at a certain moment (mmol L<sup>-1</sup>). The  $n_{TBPE}$ ,  
11  $n_{4-TBP}$ ,  $n_{2-TBP}$ ,  $n_{2,4-DTBP}$ ,  $n_{2,6-DTBP}$  and  $n_{2,4,6-TTBP}$  are the molar amounts of TBPE(*tert*-butyl  
12 phenyl ether), 4-TBP (4-*tert*-butyl phenol), 2-TBP (2-*tert*-butyl phenol), 2,4-DTBP  
13 (2,4-Di-*tert*-butyl phenol) 2,6-DTBP (2,6-Di-*tert*-butyl phenol) and 2,4,6-TTBP (2,4,6-  
14 tri-*tert*-butyl phenol) in the reaction mixture, respectively.

15

16

17

18

19

20

21

22

23

24

25

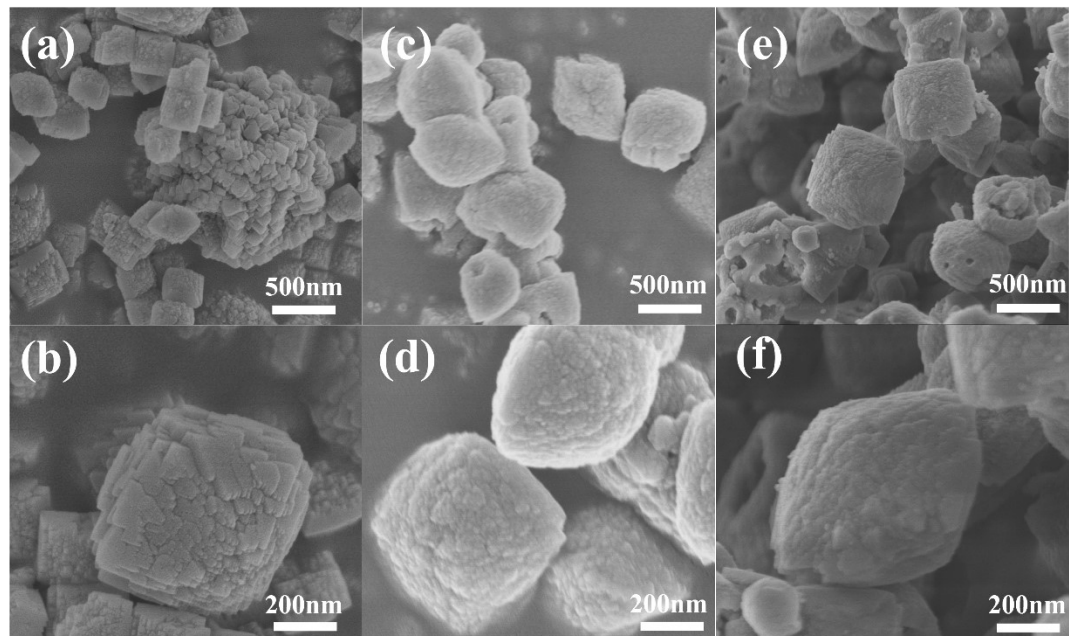
26

1

2 **Figures and Tables**

3

4

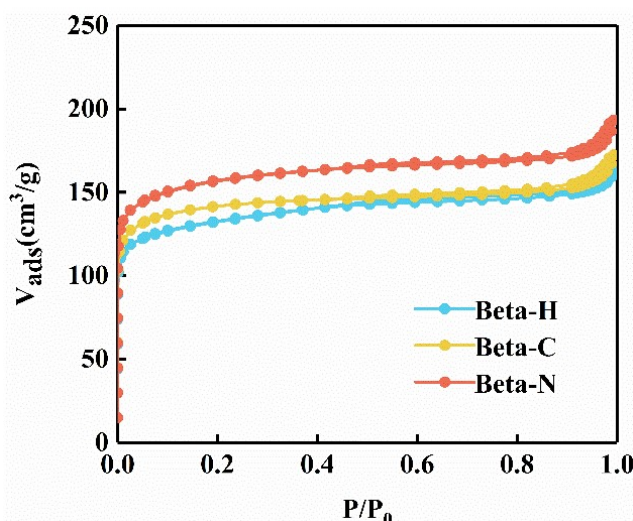


5

6 **Figure S1.** SEM images of Beta-H (a and b), Beta-C (c and d), Beta-N (e and f).

7

8



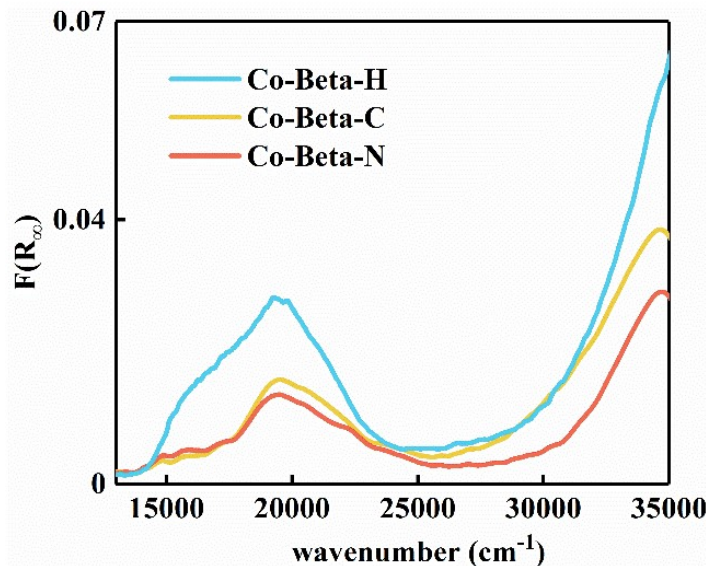
9

10 **Figure S2.** Nitrogen adsorption-desorption isotherms of the obtained Beta zeolites.

11

12

1  
2  
3

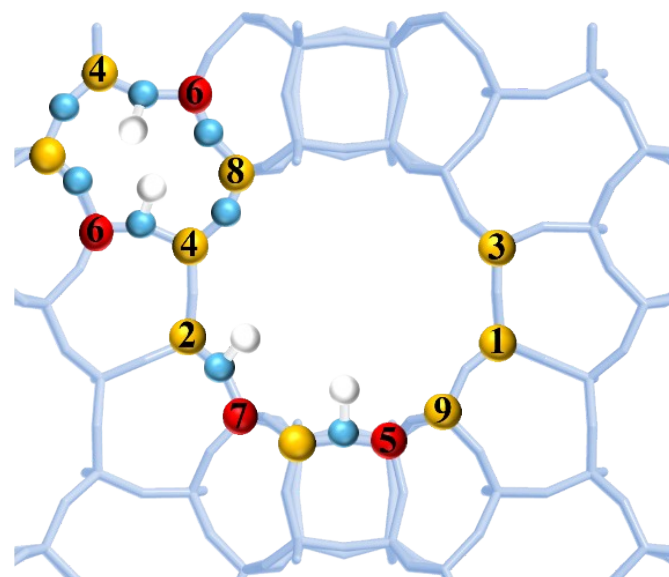


4

5 **Figure S3.** UV-vis spectra of different dehydrated Co-Beta zeolites.

6 **Note:** The absorption intensity is calculated by the Schuster Kubelka Munk equation<sup>5, 6</sup>,  $F(R_\infty) =$   
7  $(1-R_\infty)^2/2R_\infty$ .

8



9  
10 **Figure S4.** Representation of Beta zeolite framework in the [010] axis with nine different T-  
11 sites substituted by  $Al^{3+}$  ion (Si yellow, Al red, O blue, H white).  
12

1  
2  
3

4  
5

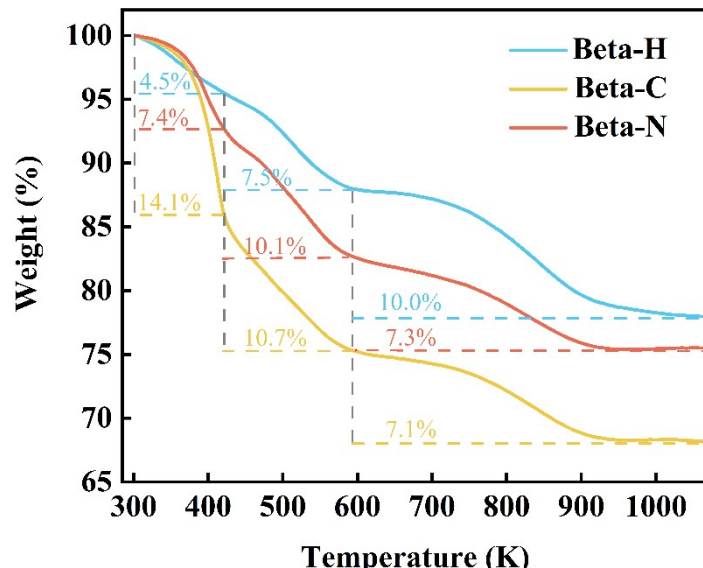
6

7 **Figure S5.** Product distributions with time-on-stream over (a) Beta-H, (b) Beta-C and (c) Beta-N,  
8 respectively.

9  
10  
11  
12  
13  
14

1

2



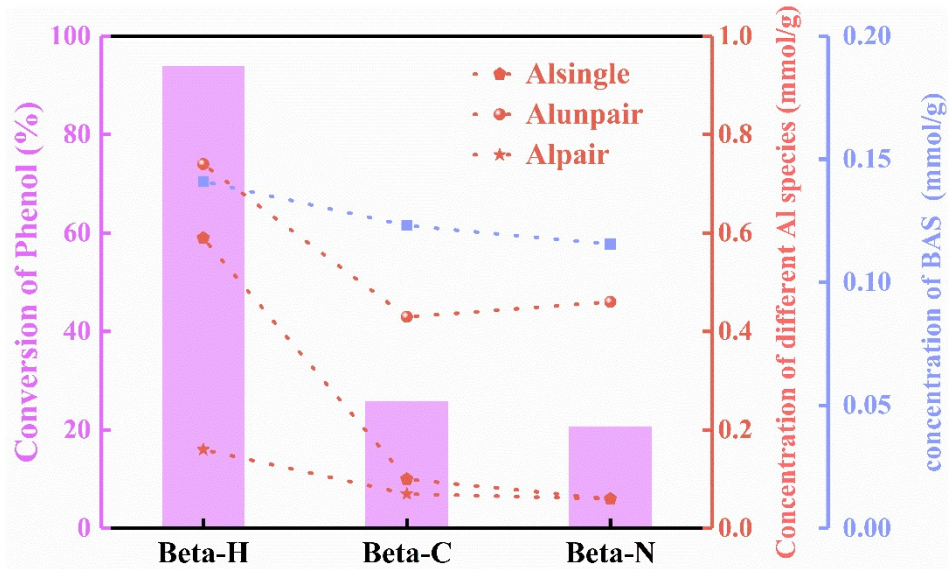
3

4

**Figure S6.** Thermogravimetric (TG) curves of various spent Beta zeolites.

5

6



7

8

**Figure S7.** Quantitative relationship between concentrations of different aluminum species and Brønsted acid sites (BAS) and phenol conversion(all provided data were evaluated at 353 K and 1 h, with a ratio of phenol and *tert*-butanol to 2:1)

9

10

11

12

1

2

3

**Table S1.** Acid density of Beta zeolite catalysts

Catalyst	Acidity <sup>a</sup> (mmol g <sup>-1</sup> )		
	Weak acid sites <sup>b</sup>	Strong acid sites <sup>c</sup>	Total acid sites <sup>d</sup>
Beta-H	1.18	0.72	1.90
Beta-C	0.92	0.49	1.41
Beta-N	0.93	0.46	1.39

<sup>a</sup> Measured by NH<sub>3</sub>-TPD.<sup>b</sup> The density of weak acid sites are measured at 323–543 K.<sup>c</sup> The density of strong acid sites are measured at 543–873 K.<sup>d</sup> The total density of acid sites = the density of weak acid sites + the density of strong acid sites.

4

5

**Table S2.** The distribution of Brønsted acid sites in Beta zeolites

Catalyst	B <sub>total</sub> <sup>a</sup> (mmol g <sup>-1</sup> )	B <sub>a&amp;b</sub> <sup>b</sup> (mmol g <sup>-1</sup> )	B <sub>c</sub> <sup>c</sup> (mmol g <sup>-1</sup> )	B <sub>a&amp;b</sub> /B <sub>total</sub> (%)
Beta-H	0.141	0.107	0.034	76
Beta-C	0.123	0.073	0.050	59
Beta-N	0.116	0.058	0.058	50

<sup>a</sup> The concentration of total Brønsted acid sites is measured by the Py-IR spectra.<sup>b</sup> The concentration of Brønsted acid sites in the channels along the *a* and *b* axis is determined by FT-IR spectra of adsorbed 2,4,6-trimethylpyridine.<sup>c</sup> The concentration of Brønsted acid sites in the channel along the *c* axis is calculated by B<sub>c</sub> = B<sub>total</sub> - B<sub>a&b</sub>.

6 **Note:** Pyridine molecules can enter into all channels of Beta zeolite along the *a*, *b* and *c* axis to  
 7 determine the total Brønsted acid sites of catalysts, while the 2,4,6-trimethylpyridine with a size of  
 8 6.2 × 5.6 Å can only access the pore channels along the *a* and *b* axis.

9

10

**Table S3.** Coke deposit of resultant Beta zeolites.

Catalyst	sample weight (mg)	soft coke <sup>a</sup> (g/g <sup>0</sup> cat) × 10 <sup>-2</sup>	hard coke <sup>b</sup> (g/g <sup>0</sup> cat) × 10 <sup>-2</sup>	Average coke rate <sup>c</sup> (mg/g <sup>0</sup> · h <sup>-1</sup> cat)
Beta-H	4.5	7.5	10.0	2.56
Beta-C	5.3	10.7	7.1	2.09
Beta-N	4.6	10.1	7.3	1.95

<sup>a</sup> The weight loss from 423 to 593 K.<sup>b</sup> The weight loss from 593 to 1073 K.<sup>c</sup> Average coke rate = the weight of hard coke/time.

11

12

## 2 References

- 3 (1) Huang, Y. Q.; Wang, M. N.; Huang, Y.; Shang, J.; Liu, B. Y. Mesoporous Beta zeolites with  
4 controlled distribution of Brnsted acid sites for alkylation of benzene with cyclohexene.  
5 *Results. Eng.*, **2023**, 19,101377.
- 6 (2) Jiang, H. Y.; Zhang, Z.; Li, X.; Zeng, X. X.; Pu, T.; Liu, B. Y. Selective alkylation of phenol  
7 and *tert*-butanol using Zr-containing Beta zeolite. *J. Mater. Chem. A*, **2025**, 13, 7882-7891.
- 8 (3) Sazama, P.; Tabor, E.; Klein, P.; Wichterlová, B.; Sklenak, S.; Mokrzycki, L.; Pashkkova,  
9 V.; Ogura, M.; Dědeček, J. Al-rich beta zeolites. Distribution of Al atoms in the framework  
10 and related protonic and metal-ion species. *J. Catal.*, **2016**, 333, 102-114.
- 11 (4) Liu, B. Y.; Zhang, J. W.; Huang, Y. Q.; Xiong, F.; Luo, R. C. Defect-designed ZSM-12  
12 zeolites for alkylation of phenol with *tert*-butyl alcohol. *Mol. Catal.*, **2022**, 519, 112144.
- 13 (5) Dědeček, J.; Čapek, L.; Kaucký, D.; Sobalík, Z.; Wichterlová, B. Siting and Distribution of  
14 the Co Ions in Beta Zeolite: A UV–Vis–NIR and FTIR Study. *J. Catal.*, **2002**, 211, 198-  
15 207.
- 16 (6) Čapek, L.; Dědeček, J.; Sazama, P.; Wichterlová, B. The decisive role of the distribution of  
17 Al in the framework of beta zeolites on the structure and activity of Co ion species in  
18 propane-SCR-NO<sub>x</sub> in the presence of water vapour. *J. Catal.*, **2010**, 272, 44-54.